

Phonon scattering in nanoscale systems: Lowest order expansion of the current and power expressions

Magnus Paulsson, Thomas Frederiksen, Mads Brandbyge

MIC – Department of Micro and Nanotechnology, NanoDTU, Technical University of
Denmark, Ørsteds Plads, Bldg. 345E, DK-2800 Lyngby, Denmark

E-mail: mpn@mic.dtu.dk

Abstract. We use the non-equilibrium Green's function method to describe the effects of phonon scattering on the conductance of nano-scale devices. Useful and accurate approximations are developed that both provide (i) computationally simple formulas for large systems and (ii) simple analytical models. In addition, the simple models can be used to fit experimental data and provide physical parameters.

1. Introduction

Since the late 1960s, inelastic effects in metal—insulator—metal systems have drawn a lot of attention both experimentally and theoretically [1, 2, 3]. In recent years inelastic effects are studied intensively with the scanning tunneling microscope (STM) [4, 5]. This has allowed the chemical identification of species under an STM tip by detecting its vibrational signature in the tunneling conductance. More recently these effects have also been investigated in the high-conductance regime with atomic-scale conductors strongly coupled to the electrodes. Agraït and co-workers used a cryogenic STM to create a freestanding atomic gold wire between the tip and substrate and, further, performed point-contact spectroscopy measurements [6]. The observed spectra displayed symmetric drops in the conductance at threshold voltages characteristic for phonons, and were found to be very sensitive to the atomic configuration. Experiments along the same lines were performed on contacted hydrogen molecules using a break-junction setup by Smit and co-workers [7].

Theoretical models of inelastic scattering has previously been developed with many-body theory in the Coulomb blockade regime [8], single-particle first-order perturbation approaches [9], i.e., “Fermi's golden rule” (FGR), as well as calculations to infinite order based on the self-consistent Born approximation (SCBA) combined with non-equilibrium Green's functions (NEGF) [10, 11]. In this chapter, we provide a more detailed description of the latter approach and the approximations we have presented previously [12]. These approximations provide computationally simple models that can be used to model large systems using ab-initio methods, i.e., molecular systems. In addition, simple models are derived that provide intuitive understanding as well as analytical expressions which allow for simple fitting to experimental data.

2. Methodology

To describe our device, e.g., an atomic gold wire connected to electrodes, the Hamiltonian is divided into contacts and device subspaces in which the scattering Hamiltonian reads:

$$\begin{aligned}
H_0 = & \sum_{\alpha,\beta \in L} H_{\alpha\beta}^L c_{\alpha}^{\dagger} c_{\beta} + \sum_{\alpha,\beta \in D} H_{\alpha\beta}^D c_{\alpha}^{\dagger} c_{\beta} + \sum_{\alpha,\beta \in R} H_{\alpha\beta}^R c_{\alpha}^{\dagger} c_{\beta} + \\
& + \sum_{\alpha \in D, \beta \in L} \left(\tau_{\alpha\beta}^{\text{DL}} c_{\alpha}^{\dagger} c_{\beta} + \text{h.c.} \right) + \sum_{\alpha \in D, \beta \in R} \left(\tau_{\alpha\beta}^{\text{DR}} c_{\alpha}^{\dagger} c_{\beta} + \text{h.c.} \right), \quad (1)
\end{aligned}$$

with terms from the two contacts (L, R), the device subspace (D) and the coupling between the device and contacts. This one-electron scattering problem can be solved exactly using the self-energies of the contacts ($\Sigma_{L,R}^r$) in the standard way [13]. In the harmonic approximation, the electron-phonon (e-ph) interaction is given by:

$$H_{\text{e-ph}} = \sum_{\lambda \in \text{Ph}} \sum_{\alpha, \beta \in D} M_{\alpha\beta}^{\lambda} c_{\alpha}^{\dagger} c_{\beta} \left(b_{\lambda}^{\dagger} + b_{\lambda} \right), \quad (2)$$

where we assume that the inelastic scattering is limited to the device subspace (D).

The steady state current and power through the systems can then be written [14]:

$$I_{\alpha} = \frac{-e}{\hbar} \int_{-\infty}^{\infty} \frac{dE}{2\pi} \text{Tr}[\mathbf{\Sigma}_{\alpha}^{<}(E) \mathbf{G}^{>}(E) - \mathbf{\Sigma}_{\alpha}^{>}(E) \mathbf{G}^{<}(E)], \quad (3)$$

$$P_{\alpha} = \frac{1}{\hbar} \int_{-\infty}^{\infty} \frac{dE}{2\pi} E \text{Tr}[\mathbf{\Sigma}_{\alpha}^{<}(E) \mathbf{G}^{>}(E) - \mathbf{\Sigma}_{\alpha}^{>}(E) \mathbf{G}^{<}(E)], \quad (4)$$

where boldface notation represents matrices in the electronic device subspace, and the various Green's functions are given by the Dyson and Keldysh equations:

$$\mathbf{G}^r(E) = \mathbf{G}_0^r(E) + \mathbf{G}_0^r(E) [\mathbf{\Sigma}_L^r(E) + \mathbf{\Sigma}_R^r(E) + \mathbf{\Sigma}_{\text{ph}}^r(E)] \mathbf{G}^r(E), \quad (5)$$

$$\mathbf{G}^{\lessgtr}(E) = \mathbf{G}^r(E) [\mathbf{\Sigma}_L^{\lessgtr}(E) + \mathbf{\Sigma}_R^{\lessgtr}(E) + \mathbf{\Sigma}_{\text{ph}}^{\lessgtr}(E)] (\mathbf{G}^r(E))^{\dagger}. \quad (6)$$

We use the zero'th order phonon Green's functions to express the phonon self-energies (to the electrons) in the device subspace. Neglecting the polaron term (discussed below) [15, 16]:

$$\mathbf{\Sigma}_{\text{ph}}^{\lessgtr}(E) = \sum_{\lambda} \mathbf{M}_{\lambda} \left[(n_{\lambda} + 1) \mathbf{G}^{\lessgtr}(E \pm \hbar\omega_{\lambda}) + n_{\lambda} \mathbf{G}^{\lessgtr}(E \mp \hbar\omega_{\lambda}) \right] \mathbf{M}_{\lambda}, \quad (7)$$

$$\mathbf{\Sigma}_{\text{ph}}^r(E) = \frac{1}{2} \left(\mathbf{\Sigma}_{\text{ph}}^{>} - \mathbf{\Sigma}_{\text{ph}}^{<} \right) - \frac{i}{2} \mathcal{H} \left[\mathbf{\Sigma}_{\text{ph}}^{>} - \mathbf{\Sigma}_{\text{ph}}^{<} \right]. \quad (8)$$

Here, \mathbf{M}_{λ} is the e-ph coupling matrix for phonon mode λ occupied by n_{λ} phonons with energy $\hbar\omega_{\lambda}$. The lesser/greater self-energy matrices $\mathbf{\Sigma}_{\text{ph}}^{\lessgtr}$ are given by two terms corresponding to absorption/emission of phonon quanta. We also implicitly assume that these self-energies can be used in non-equilibrium with a bias dependent phonon occupation number $n_{\lambda}(V)$. The retarded phonon self-energy is obtained from the lesser/greater parts Eq. (8) using the Hilbert transform (Kramers-Kronig relation):

$$\mathcal{H} [g(x')] (x) = \frac{1}{\pi} \mathcal{P} \int g(x') / (x - x') dx'. \quad (9)$$

Traditionally these equations are solved numerically by calculating the self-energies from which the various Green's functions are found. The SCBA solution is often favored and found from iteration. However, numerical integration of Eq. (3) rapidly becomes very demanding with increasing size of the system. It is therefore important to find reasonable approximations.

2.1. Lowest order expansion (LOE)

The type of experimental measurements we focus on, i.e., nanoscale devices connected to metallic contacts, typically have a weak e-ph coupling strength. The computational difficulties can thus be resolved by (i) expanding the current and power expressions (Eqs. (3)-(4)) to second order in the e-ph couplings and (ii) approximating the contact broadening and non-interacting retarded Green's function as energy independent matrices. In a more mathematical language we use the following approximations:

$$\mathbf{G}_0^r(E) \approx \mathbf{G}_0^r(E_F), \quad (10)$$

$$\mathbf{\Gamma}_{L,R}(E) \approx \mathbf{\Gamma}_{L,R}(E_F), \quad (11)$$

where $\Gamma = i(\Sigma - \Sigma^\dagger)$ is the contact broadening. These approximations seems to be valid for a large number of nanoscale devices since they are reasonable if (i) the electron spends a short time compared to the phonon scattering time in the device, (ii) the contacts are metallic with slowly varying density of states, and (iii) the Fermi energy is either far away from a resonance or the broadening by the contacts is large to ensure Eq. (10).

With these approximations, the current and power expressions can be expanded to lowest order (second) in the e-ph coupling and the integration over energy performed analytically. After lengthy and tedious algebra, the power dissipated into the phonon system P^{LOE} can be written:

$$P^{\text{LOE}} = \sum_{\lambda} \frac{(\hbar\omega_{\lambda})^2}{\pi\hbar} (n_B(\hbar\omega_{\lambda}) - n_{\lambda}) \text{Tr} [\mathbf{M}_{\lambda}\mathbf{A}\mathbf{M}_{\lambda}\mathbf{A}] + \mathcal{P}(V, \hbar\omega_{\lambda}, T) \text{Tr} [\mathbf{M}_{\lambda}\mathbf{G}\mathbf{\Gamma}_L\mathbf{G}^{\dagger}\mathbf{M}_{\lambda}\mathbf{G}\mathbf{\Gamma}_R\mathbf{G}^{\dagger}], \quad (12)$$

$$\mathcal{P} = \frac{\hbar\omega}{\pi\hbar} \frac{(\cosh(\frac{eV}{kT}) - 1) \coth(\frac{\hbar\omega}{2kT}) \hbar\omega - eV \sinh(\frac{eV}{kT})}{\cosh(\frac{\hbar\omega}{kT}) - \cosh(\frac{eV}{kT})}, \quad (13)$$

where n_B is the Bose-Einstein distribution which appears naturally from the integration of the Fermi functions of the electrons in the contacts. Here, $\mathbf{G} = \mathbf{G}_0^r(E_F)$, $\mathbf{\Gamma}_{L,R} = \mathbf{\Gamma}_{L,R}(E_F)$, and $\mathbf{A} = i(\mathbf{G} - \mathbf{G}^{\dagger})$ are the non-interacting, i.e., without phonon interactions, retarded Green's function, the broadening by the contacts, and spectral function at E_F , respectively.

From Eq. (12) we see that the power can be decomposed into terms corresponding to the individual phonon modes. We also note that the first term describes the power balance between the electron and phonon systems (at zero bias) with an electron-hole damping rate $\gamma_{\text{eh}}^{\lambda} = \omega_{\lambda}/\pi \text{Tr} [\mathbf{M}_{\lambda}\mathbf{A}\mathbf{M}_{\lambda}\mathbf{A}]$. This is in fact equivalent to the Fermi's golden rule expression [17]. The second term is even in bias and gives the phonon absorption/emission at non-equilibrium; it is negligible at low bias ($eV \ll \hbar\omega$), turns on at the phonon energy and becomes linear in voltage at high bias ($eV \gg \hbar\omega$) where phonon scattering is not blocked by the Pauli principle.

Using the same approximations, the current through the device I^{LOE} is given by:

$$I^{\text{LOE}} = \frac{e^2V}{\pi\hbar} \text{Tr} [\mathbf{G}\mathbf{\Gamma}_R\mathbf{G}^{\dagger}\mathbf{\Gamma}_L] + \sum_{\lambda} \mathcal{I}^{\text{Sym}}(V, \hbar\omega_{\lambda}, T, n_{\lambda}) \text{Tr} \left[\mathbf{G}^{\dagger}\mathbf{\Gamma}_L\mathbf{G} \left\{ \mathbf{M}_{\lambda}\mathbf{G}\mathbf{\Gamma}_R\mathbf{G}^{\dagger}\mathbf{M}_{\lambda} + \frac{i}{2} \left(\mathbf{\Gamma}_R\mathbf{G}^{\dagger}\mathbf{M}_{\lambda}\mathbf{A}\mathbf{M}_{\lambda} - \text{h.c.} \right) \right\} \right] + \sum_{\lambda} \mathcal{I}^{\text{Asym}}(V, \hbar\omega_{\lambda}, T) \text{Tr} \left[\mathbf{G}^{\dagger}\mathbf{\Gamma}_L\mathbf{G} \left\{ \mathbf{\Gamma}_R\mathbf{G}^{\dagger}\mathbf{M}_{\lambda}\mathbf{G} (\mathbf{\Gamma}_R - \mathbf{\Gamma}_L) \mathbf{G}^{\dagger}\mathbf{M}_{\lambda} + \text{h.c.} \right\} \right], \quad (14)$$

$$\mathcal{I}^{\text{Sym}} = \frac{e}{\pi\hbar} \left(2eVn_{\lambda} + \frac{\hbar\omega_{\lambda} - eV}{e \frac{\hbar\omega_{\lambda} - eV}{kT} - 1} - \frac{\hbar\omega_{\lambda} + eV}{e \frac{\hbar\omega_{\lambda} + eV}{kT} - 1} \right), \quad (15)$$

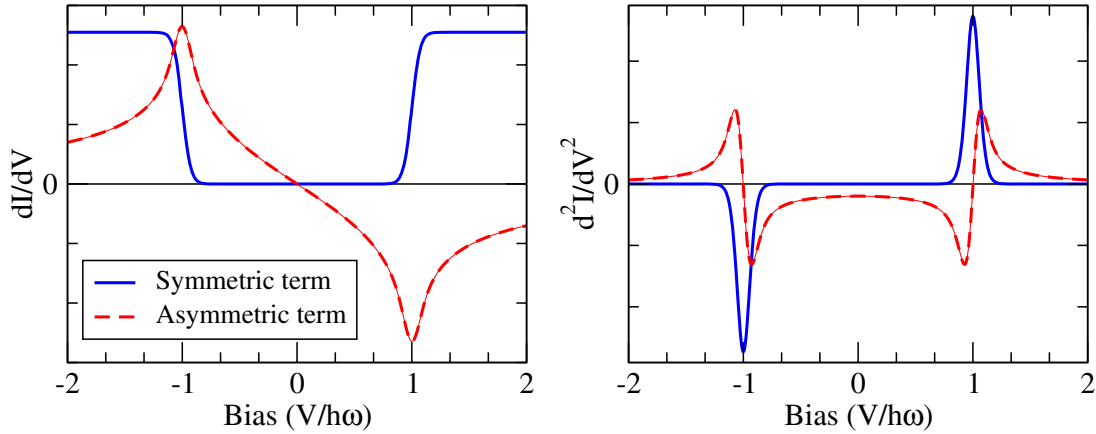


Figure 1. Universal functions (Eqs. (15)-(16)) giving the phonon contribution to the current. The differential conductance dI/dV and the second derivative signals are shown for one phonon mode with the bias in units of the phonon energy at a temperature $kT = 0.025 \hbar\omega$. For the symmetric term, the FWHM of the second derivative peak is approximately $5.4 kT$ [2].

$$\mathcal{I}^{\text{Asym}} = \frac{e}{2\pi\hbar} \int_{-\infty}^{\infty} [n_F(E) - n_F(E - eV)] \mathcal{H} [n_F(x + \hbar\omega_\lambda) - n_F(x - \hbar\omega_\lambda)] dE, \quad (16)$$

where n_F is the Fermi function, the bias is defined via $eV = \mu_R - \mu_L$, and the conductance quantum $G_0 = e^2/\pi\hbar$ appears naturally. We note that these expressions are current conserving in contrast to the first order Born approximation (SCBA is also current conserving).

The current expression retains the structure of the Landauer expression (first term of Eq. (14)) and gives correction terms for each phonon mode. The phonon terms can in turn be divided into a “symmetric” part \mathcal{I}^{Sym} where the differential conductance dI/dV is even in bias, and an “asymmetric” part containing the Hilbert transform $\mathcal{I}^{\text{Asym}}$ which yields an odd contribution. We note that the simple factorization into terms depending on the electronic structure at E_F and *universal* functions \mathcal{I}^{Sym} and $\mathcal{I}^{\text{Asym}}$ yields the line-shape of the inelastic signals, see Fig. 1. Whether the conductance increases or decreases due to phonon scattering depends on the sign of the traces in Eq. (14) and will be discussed further below. Examination of the “asymmetric” term in Eq. (14) shows that it is zero for symmetric systems. Although experimentally measured conductances contain asymmetric signals, the size of the asymmetry is usually small in the published curves. At the present time it is therefore unclear if they are caused by phonons or other effects.

The different terms of the traces in Eq. (14) can also be interpreted. The first term in the symmetric contribution comes from direct inelastic scattering while the other terms are corrections to the elastic conductance through the device. This is also evident in the power expression Eq. (12), where only the inelastic scattering term is present since corrections to the elastic conductance give no dissipation of energy.

We have also derived the LOE expansion of the current and power including the polaron term in the self-energy (i.e., Hartree term of the phonon self-energy). However, this result has been omitted from this publication since the polaron term does not contribute to the power expression (the polaron term only gives a correction to the elastic scattering). In addition, the bias dependence of the corrections to the current are proportional to V , and V^2 . Thus they give no additional signals in the LOE at the phonon energy.

As we have shown previously heating of the phonon system should be considered which makes

the number of phonons n_λ bias dependent [11]. The simplest way to include non-equilibrium heating is to write down a rate equation, including an external damping rate γ_d^λ of the phonons:

$$\dot{n}_\lambda = \frac{P_\lambda^{\text{LOE}}}{\hbar\omega} + \gamma_d^\lambda (n_B(\hbar\omega_\lambda) - n_\lambda), \quad (17)$$

where P_λ^{LOE} is the power dissipated into the individual phonon modes.¹ The steady state occupation n_λ is easily found. Substituting the result into Eqs. (14)-(16) gives a computationally simple but powerful formula for the current through the device which also includes heating of the phonon system. However, the inelastic signal in d^2I/dV^2 calculated from Eq.(14) will not show the correct width, since the phonons Green's functions used in the current calculation are undressed by the interaction with the electrons.

3. Simple models

The intimidating formulas (Eqs. (12)-(14)) are difficult to interpret and we find it important to use simpler models to illustrate the physics. Below we present two such models which have been used to fit experimental data, see Ref. [12].

3.1. One level model

To gain further insight, we consider a single electronic level with symmetric contacts $\Gamma = \Gamma_L = \Gamma_R$ coupled to one phonon mode. Rewriting the equations using the transmission probability $\tau = |G|^2\Gamma^2$ and defining the electron-hole damping rate from the first term of Eq. (12) $\gamma_{\text{eh}} = 4(\omega/\pi) M^2\tau^2/\Gamma^2$, we obtain:

$$P_{\text{one}}^{\text{LOE}} = \gamma_{\text{eh}} \hbar\omega (n_B(\hbar\omega) - n) + \frac{\gamma_{\text{eh}}}{4} \frac{\pi\hbar}{\hbar\omega} \mathcal{P}, \quad (18)$$

$$I_{\text{one}}^{\text{LOE}} = \frac{e^2}{\pi\hbar} \tau V + e\gamma_{\text{eh}} \frac{1 - 2\tau}{4} \frac{\pi\hbar}{e\hbar\omega} \mathcal{I}^{\text{Sym}}. \quad (19)$$

The conductance and d^2I/dV^2 for this model is shown in Fig. 2 for two cases corresponding to high ($\tau \approx 1$) and low transmission ($\tau \ll 1$). For the high conductance example, left part of figure, we note that the effect of phonon scattering is to decrease the conductance while for the low conductance example (right part), the phonon helps the electron through the device. From Eq. (19) this reflects the $1 - 2\tau$ term, the conductance will increase due to phonon scattering for low conductance systems ($\tau < 1/2$) and decrease for highly conducting systems ($\tau > 1/2$). This reinforces the point that the LOE approach directly provides the sign of the conductance change in contrast to Fermi golden rule approaches where careful consideration of the occupancy of initial and final states is required [9].

The number of phonons present in the system affects the conductance through the universal function Eq. (15), which shows that the conductance is simply shifted by the number of phonons. The fact that the number of phonons affect the conductance equally much (independent of bias voltage) can be understood from the fact that an increase in the number of phonons gives increasing phonon absorption at low bias and enhanced phonon emission at high bias (stimulated emission). The bias dependence in these two terms cancel and gives overall a bias independent effect.

Heating: The phonon emission at high bias will heat a nanoscale device unless the excess phonons are allowed to relax into the environment. To model this we use Eq. (17). Solving for the number of phonons we find the extra slope in the conductance at high bias seen in Fig. 2

¹ For weak e-ph interaction, the division of power into the individual phonon modes is straightforward from Eq. (12).

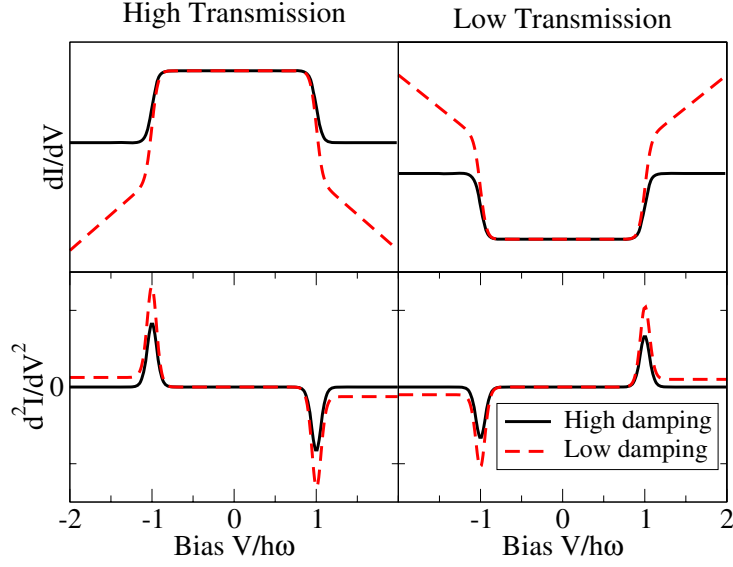


Figure 2. Conductance (top) and d^2I/dV^2 (bottom) for a high conductance model (left) and low conductance model (right). The damping rate of the phonons, i.e., escape of phonons into the contacts, was set to infinity (zero) for the high (low) damping case.

(for the low damping case). The interpretation is straight forward, the phonon emission starting at a bias equal to the phonon frequency heats the system and increases the effect of phonon scattering. Note that the heating gives a bias dependent effect on the conductance in contrast to the effect of the number of phonons described in the previous paragraph.

In the case of asymmetric coupling, $\Gamma_L = \Gamma - \Delta\Gamma/2$, $\Gamma_R = \Gamma + \Delta\Gamma/2$, we obtain an additional asymmetric correction which gives an odd (in bias) contribution to the conductance:

$$I_{\text{one}}^{\text{LOE}} = \frac{e^2}{\pi\hbar}\tau V + e\gamma_{\text{eh}} \frac{1 - (\Delta\Gamma/2\Gamma) - 2\tau}{4} \frac{\pi\hbar}{e\hbar\omega} \mathcal{I}^{\text{Sym}} + \gamma_{\text{eh}}\tau \left(\frac{\Delta\Gamma}{2\Gamma}\right) \left(\frac{E_F - \varepsilon_0}{2\Gamma}\right) \frac{\pi\hbar}{e\hbar\omega} \mathcal{I}^{\text{Asym}}. \quad (20)$$

It is interesting to note that the sign of the asymmetric contribution depends on the position of the resonance level, ε_0 , relative to the Fermi energy. This makes it, in principle, possible to determine whether a resonance is filled or empty provided that it is known to which electrode the weaker coupling occurs ($\Gamma_L < \Gamma_R$). A typical asymmetric example occurs in the case of STM where one electrode is a tunneling contact where the coupling can be varied by mechanically separating the tip from the device.

3.2. Gold chains

The electronic structure of atomic gold chains are qualitatively different from that of a one level model. In addition, only the alternating bond length mode (ABL) in a gold chain backscatters the electrons due to momentum conservation [11]. To derive an alternating bond length model we use the e-ph matrix for an ABL phonon mode [11]:

$$M_{\alpha,\beta} = M (-1)^\beta (\delta_{\alpha,\beta-1} + \delta_{\alpha,\beta+1}), \quad (21)$$

where δ is the Kronecker delta. Using the retarded Green's function for a half-filled perfectly transmitting one-dimensional chain we obtain:

$$P_{\text{ABL}}^{\text{LOE}} = \gamma_{\text{eh}} \hbar\omega [n_B(\hbar\omega) - n] + \frac{\gamma_{\text{eh}}}{2} \frac{\pi\hbar}{\hbar\omega} \mathcal{P}, \quad (22)$$

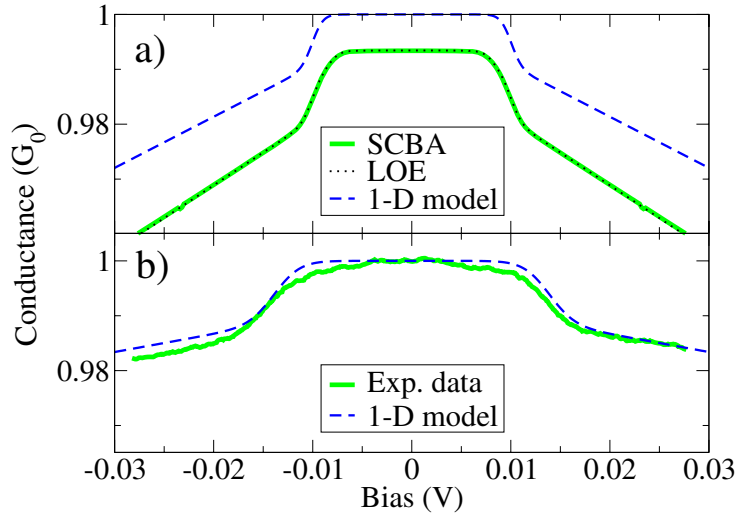


Figure 3. Conductance characteristics of an atomic Au wire. a) Comparison between the SCBA results, LOE (Eq. (14)) and ABL (Eq. (23)) expressions including heating ($\gamma_d = 0$ and $T = 4.2\text{K}$). The parameters for the ABL model were extracted directly from the DFT calculations, $\gamma_{eh} = 5.4 \times 10^{10} \text{s}^{-1}$ and $\hbar\omega = 13.4 \text{meV}$. b) ABL model fitted to experimental data from Ref. [6], $\gamma_{eh} = 12 \times 10^{10} \text{s}^{-1}$, $\gamma_d = 36 \times 10^{10} \text{s}^{-1}$, $T = 10\text{K}$ and $\hbar\omega = 13.8 \text{meV}$.

$$I_{\text{ABL}}^{\text{LOE}} = \frac{e^2}{\pi\hbar} V - \frac{e\gamma_{eh}}{2} \frac{\pi\hbar}{e\hbar\omega} \mathcal{I}^{\text{Sym}}, \quad (23)$$

where the only differences to the one-level model are that $\tau = 1$ (perfect transmission) and a factor of two reflecting the different amounts of forward and backward scattering in the two models. In other words, momentum conservation forbids forward scattering for the ABL model, while the one level model has equal amounts of forward and backward scattering since the phonon couples equally to all scattering states. The resulting conductance is shown in Fig. 3, where the parameters of the simple model were calculated directly from density functional theory as described in Ref. [11] and [12].

4. First principles methods

To verify the accuracy of the LOE approach, the LOE approximation is compared to the full SCBA solution for a four atom gold wire, see Fig. 3, as well as the ABL model. The Hamiltonian, phonon frequencies, and e-ph couplings were calculated using density functional theory as described previously [11]. For the gold wire, the excellent agreement between the approximate treatment and the full SCBA solution is not unexpected since the density of states for a gold surface around the Fermi energy is almost completely composed of the s -band with nearly constant density of states. In addition, the electrons is carried through the wire by one s -channel with a nearly constant transmission across a wide energy range. The e-ph interaction is also weak since the electrons rapidly cross the wire and there is no resonances trapping the electron.

The computationally much simpler LOE equations were solved in less than a minute on a regular PC, compared to several hours for the SCBA calculations. The LOE approach thus opens up the possibility to study inelastic scattering with first principles methods for large systems, e.g., organic molecules. However, great care has to be taken to check the validity of the LOE approximation since molecules may have rapidly varying transmission near the Fermi energy if

there are narrow resonances close by.

5. Summary

The simple models derived in Sec. 3 give intuitively appealing descriptions of phonon scattering. They provide understanding of the important questions, (i) whether phonon scattering leads to an increase or decrease of the conductance, and (ii) how non-equilibrium heating influences the conductance increase/decrease. In addition, the full lowest order expansion results (Eqs. (12)-(14)) provide a computationally fast method that may be used for large systems where the SCBA approximation is infeasible.

Acknowledgments

Discussions with Prof. A.-P. Jauho are gratefully acknowledged. This work, as part of the European Science Foundation EUROCORES Programme SASMEC, was supported by funds from the SNF and the EC 6th Framework Programme. Computational resources were provided by the Danish Center for Scientific Computations (DCSC).

References

- [1] C. B. Duke. *Tunneling in Solids*, volume Supplement 10 of *Solid State Physics ed. by H. Ehrenreich, F. Seitz, and D. Turnbull*, page 209. Academic, New York, 1969.
- [2] P. K. Hansma. Inelastic electron-tunneling. *Phys. Rep.*, 30:145, 1977.
- [3] C. Caroli, D. Saint-James, R. Combescot, and P. Nozières. Direct calculation of tunnelling current : Electron-phonon interaction effects. *J. of Phys. C*, 5(1):21-&, 1972.
- [4] B. C. Stipe, M. A. Rezaei, and W. Ho. Single-molecule vibrational spectroscopy and microscopy. *Science*, 280(5370):1732–1735, 1998.
- [5] N. Lorente and M. Persson. Theory of single molecule vibrational spectroscopy and microscopy. *Phys. Rev. Lett.*, 85(14):2997–3000, 2000.
- [6] N. Agrait, C. Untiedt, G. Rubio-Bollinger, and S. Vieira. Onset of energy dissipation in ballistic atomic wires. *Phys. Rev. Lett.*, 88(21):216803, 2002.
- [7] R. H. M. Smit, Y. Noat, C. Untiedt, N. D. Lang, M. C. van Hemert, and J. M. van Ruitenbeek. Measurement of the conductance of a hydrogen molecule. *Nature*, 419(6910):906–909, 2002.
- [8] S. Braig and K. Flensberg. Vibrational sidebands and dissipative tunneling in molecular transistors. *Phys. Rev. B*, 68:205324, 2003.
- [9] M. J. Montgomery, J. Hoekstra, T. N. Todorov, and A. P. Sutton. Inelastic current-voltage spectroscopy of atomic wires. *J. of Phys.-Cond. Mat.*, 15(4):731–742, 2003.
- [10] M. Galperin, M. A. Ratner, and A. Nitzan. On the line widths of vibrational features in inelastic electron tunneling spectroscopy. *Nano Lett.*, 4(9):1605–1611, 2004.
- [11] T. Frederiksen, M. Brandbyge, N. Lorente, and A.-P. Jauho. Inelastic scattering and local heating in atomic gold wires. *Phys. Rev. Lett.*, 93:256601, 2004.
- [12] M. Paulsson, T. Frederiksen, and M. Brandbyge. Modeling inelastic phonon scattering in atomic- and molecular-wire junctions. *Phys. Rev. B*, 72:201101(R), 2005.
- [13] S. Datta. *Electronic Transport in Mesoscopic Systems*. Cambridge University Press, Cambridge, UK, 1995.
- [14] Y. Meir and N. S. Wingreen. *Phys. Rev. Lett.*, 68:2512, 1992.
- [15] H. Haug and A.-P. Jauho. *Quantum kinetics in transport and optics of semiconductors*. Springer-Verlag, Berlin, 1996.
- [16] A. Pecchia and A. Di Carlo. Atomistic theory of transport in organic and inorganic nanostructures. *Rep. Prog. Phys.*, 67(8):1497, 2004.
- [17] B. N. J. Persson and M. Persson. Damping of vibrations in molecules adsorbed on a metal-surface. *Surf. Sci.*, 97(2-3):609–624, 1980.